J. Phys. A: Math. Gen. 23 (1990) 3835–3859. Printed in the UK

A network of oscillators*

L F Abbott
Physics Department, Brandeis University, Waltham, MA 02254, USA

Received 11 December 1989

Abstract. A model of neuronal behaviour capable of accounting for the oscillatory, plateau and rebound properties of biological neurons is derived, discussed and analysed. The model is based on a piecewise linear form of the FitzHugh–Nagumo equations, but reduces to a set of maps very similar to those of the Hopfield model. In particular, the binary description of individual neurons and the well studied form of the synaptic current $\sum J_{ij}S_j$ are preserved, although the model is capable of reproducing behaviours on the slow timescales characteristic of plateau and oscillation. By coupling two model cells together a mutually inhibitory or half-centred oscillator and an oscillator, fixed-phase follower pairs are constructed. The behaviour of a network of oscillatory cells is analysed with particular attention to phase-locking. The response of a single cell to a square wave input provides a mean-field approximation for large networks. This approach is compared with the results of a phase-coupling description of the oscillators. The network of oscillators discussed can be used to construct associative memories in which the signal for memory recall is not fixed-point behaviour but phase locking. The performance and capacity of such phase-locking memories is analysed.

1. Introduction

Modelling neuronal behaviour involves a continual competitive interplay between the simplicity needed for mathematical tractability and the complexity required for biological accuracy. Researchers with an analytic bent have frequently opted for an extremely simple model based on binary neurons with essentially instantaneous dynamics that leaves many biologists cold. On the other hand, more biologically motivated models are often so complex that they provide little analytic or intuitive insight into the dynamics they simulate. The goal of model building is to provide something between these extremes. The model discussed here is capable of reproducing many of the more complex features of neuronal behaviour while retaining the simplicity needed for both mathematical analysis and intuitive insight.

The simplest and most thoroughly analysed mathematical network is the Hopfield model [1]. In this model, an individual neuron is treated as a simple two-state system characterised by a binary variable which takes the value $+1$ if the neuron is firing and -1 if it is not. Similarly, a system of N interacting neurons is described by N variables S_i obeying

$$S_i = \pm 1 \qquad i = 1 \ldots N. \tag{1.1}$$

* Research supported by Department of Energy Contract DE-AC0276-ER03230.

0305-4470/90/163835+25$03.50

The behaviour of each neuron is governed by the signal it receives from other cells through synaptic connections and from possible external sources. The strength of the synaptic connection between neuron i and neuron j is given by a matrix element J_{ij}. The total current entering cell i due to the firing of other cells in the network and from external sources is

$$\tilde{I}_i = \sum_{j=1}^{N} J_{ij}(S_j + 1) + I_i^{\text{ext}} \tag{1.2}$$

with

$$J_{ii} = 0. \tag{1.3}$$

The firing or non-firing of the cell is determined by whether or not this current exceeds a certain threshold value $\tilde{\theta}_i$. Time is divided into discrete intervals of order the refractory period, a few msec, and the state of cell i at time $t + 1$ is determined by the state of the system at time t by the basic dynamic rule

$$S_i(t + 1) = \text{sgn}[\tilde{I}_i(t) - \tilde{\theta}_i]. \tag{1.4}$$

It is more convenient to absorb a constant factor from $\tilde{I}_i$ into the threshold term defining

$$\theta_i = \tilde{\theta}_i - \sum_{j=1}^{N} J_{ij} \tag{1.5}$$

and

$$I_i = \sum_{j=1}^{N} J_{ij} S_j + I_i^{\text{ext}} \tag{1.6}$$

so that

$$S_i(t + 1) = \text{sgn}[I_i(t) - \theta_i]. \tag{1.7}$$

A number of problems arise when the model discussed above is applied to biological systems. Three of the most serious are: (1) the model describes individual cells as either firing or not firing allowing for no variation or time dependence in the firing rate; (2) the synaptic current is instantaneous, independent of the membrane potential of the postsynaptic cell and only binarily dependent on the potential of the presynaptic neuron; none of these properties hold true for biological systems; (3) the response of a cell to its incoming synaptic current is essentially instantaneous. As a result, there is no possibility of any long term hysteresis or dynamic dependence on past behaviour nor intrinsic oscillations or delays with periods much greater than the fundamental timescale of around a msec.

An enormous amount of attention has been given in modelling studies to resolving problem (1) by providing sets of differential equations to reproduce the cell membrane potential in such a way that individual action spikes are described [2]. This involves a significant complication since the description and computation of rapid spiking in the

membrane potential is quite difficult. At the same time, it is not clear that this detailed level of modelling is essential. The contribution of individual action potential spikes to overall network behaviour is not very significant. It is their integrated effect and the level of the average cell potential which is crucial. There are examples of biological networks which are capable of relatively normal functioning when action potentials are pharmacologically blocked [3]. A continuous variable describing the spiking rate as a function of time or, equivalently, the spike-averaged membrane potential is probably a sufficient description. There seems to be little need to actually model individual action potentials. In the model discussed here, the spike-averaged cell membrane potential will be available as a direct measure of the spiking rate.

The simplistic modelling of synapses discussed in problem (2) is more troubling. We might argue that for rapidly acting synapses, the synaptic time delay can be ignored. For reversal potentials which are large compared with typical membrane potentials, we can, as a first approximation, ignore the dependence on the postsynaptic cell potential as well. However, the real advantage of using the simple form (1.6) for the synaptic current is that a tremendous amount is known about how this current depends on the coupling matrix J_{ij} [4]. Here, I will take the viewpoint that this body of knowledge is too much to give up and that synaptic connections are too variable and too poorly described to provide a very realistic model of the synaptic current anyway. Therefore, (1.6) will remain unchanged. The use of this well studied form of the synaptic current allows us to apply previous results [4] on storage capacity, current strength and learning algorithms to the present model.

Probably the most severe of the three problems mentioned is (3), the instantaneous nature of the cell dynamics in the Hopfield model. Real neurons display many behaviours which reflect a slow timescale (much greater than 1 msec) [5] that are not modelled by (1.7). Such slow behaviours undoubtedly have a profound impact on network behaviour. For example, in response to a positive external current pulse a biological cell may go into the firing ($S_i = +1$) state for a time period much longer than the duration of that external pulse, a property known as plateau behaviour. When a negative current is applied for a period of time and then is quickly removed, a cell may exhibit postinhibitory rebound, a period of firing activity in response to release from negative current inhibition. Another effect of this sort is post-firing inhibition which refers to the behaviour of a cell following a prolonged firing burst. It is often more difficult to re-excite a neuron to the firing state immediately after a burst of activity than it is to excite a silent, resting cell. In addition, neurons may spontaneously oscillate between firing and non-firing states with periods up to several seconds even in the absence of external currents or interactions with other cells. All of these behaviours are characterised by a hysteresis or memory of past experience on a relatively long timescale, and none of them can be described even qualitatively by the Hopfield model. The model discussed here addresses this serious shortcoming.

An additional problem that has received considerable attention [6] concerns the description of a neuron by a single membrane potential or equivalent variable like S_i. If the different regions of the cell body are not characterised by the same potential such a description is necessarily incomplete. This problem can be circumvented by stipulating that the 'cell' being modelled is not the whole cell body but an isopotential piece of it. With this stipulation we will continue to ignore this complication.

The model will be constructed starting from a description of cell behaviour in terms of a well known set of differential equations. However, once the derivation is complete, the model will be expressed in a form very similar to the Hopfield model

especially versions of this model with time-dependent thresholds [7] and hysteresis [8]. The threshold factor will be described by an addition map. In fact, in the limit of strong synaptic currents the model behaves very much like the Hopfield model and thus, this derivation also serves to reproduce the simpler model. For smaller synaptic currents the model exhibits all of the slow timescale behaviours discussed above and can, for example, describe a network of coupled oscillatory cells. In the following I consider the behaviour of individual model neurons responding to external currents, the dynamics of coupled pairs of model neurons, and the behaviour of large, highly coupled systems of oscillators. A well studied property of the Hopfield model is associative memory, the mapping of a given input to a nearby fixed-point of the dynamics. For the networks of oscillators discussed here, the analogous behaviour is the phase locking of the oscillators in response to a recognised pattern. Throughout, the simplicity of the model allows for detailed analytic, mean-field and phase-coupling calculations even though highly non-trivial dynamical behaviours are exhibited.

2. The model

The behaviour of a cell membrane potential in response to external and synaptic currents is governed by current conservation and by properties of the membrane currents of the cell. Each membrane current is determined by a conductance and by the difference between the cell potential and the reversal potential for the particular conduction ion producing the current. A complete model would consist of the equation for current conservation along with differential equations describing all of the cell conductances as functions of time and membrane potential. Even highly simplified attempts at building such models end up being quite complicated and difficult to treat either analytically or intuitively. A well known simplifying approximation [9] is to divide the total membrane current into two pieces, one consisting of all conductances which respond rapidly, say in a time of order several msec or less, and another composed of the slow conductances responding in times ranging from tens of msec to a sec or more. The fast set of conductances is then considered to be an instantaneous function of the membrane potential thereby eliminating the entire set of differential equations for fast conductance channels. Let $F(V)$ be the fast outward membrane current at cell potential V and let U be the slow component of the membrane current. Then, by current conservation

$$C\frac{dV}{dt} = -F(V) - U + I \tag{2.1}$$

where C is the cell membrane capacitance and I is the sum of synaptic and external currents entering the cell. The current component U responds slowly to changes in the membrane potential and its behaviour has traditionally been modelled [10] using a linear first-order differential equation

$$\frac{dU}{dt} = \alpha V - \beta U. \tag{2.2}$$

If $F(V)$ is taken to be a cubic polynomial, (2.1) and (2.2) give the well known FitzHugh–Nagumo model [10] of a neuron and for appropriate choices of parameters describe a relaxation or van der Pol oscillator [11]. Here, $F(V)$ will not be a cubic

but rather will be approximated by a piecewise linear form consisting of two positive resistance regions connected by a negative resistance piece. This provides several advantages. First, a linear form provides a better description of the I–V curve of a real neuron than a cubic, at least asymptotically once the conductances have saturated. Second, the essential feature in the cubic $F(V)$ of the FitzHugh–Nagumo model is its 'N'-like shape and this is duplicated by the piecewise linear form with the negative resistance region. In addition, the piecewise linear $F(V)$ has the great advantage of leading ultimately to a differential equation which can easily be solved. To keep things reasonably simple, it is assummed that the resistance in all three linear regions of $F(V)$ has the same magnitude, although this condition could easily be dropped to provide more flexibility at the expense of two more parameters.

Normally (2.1) and (2.2) are used to describe a series of action potentials, with the slow timescale providing and determining the interspike period. Here, these equations will be employed in a completely different way. The variable V will correspond to a mean cell potential with action spikes averaged out. Action potentials will thus be ignored, and the slow timescale will provide and determine the behaviour of plateau and oscillatory phenomena. Although individual action potentials will not be described by the model, the membrane potential V provides a continuous measure of the spiking rate.

With an additional simplifying approximation, the final model can now be derived. There are three timescales relevant to the differential equations (2.1) and (2.2). The fastest of these is the timescale associated with the turning on and off of the conductances responsible for the fast component of the membrane current. Next, is the capactive time constant which governs changes in the membrane potential given by (2.1). This capacitive charging time is still very short in comparison with the third timescale, that associated with the slow membrane current through (2.2). It is therefore reasonable to treat the capacitive charging process as well as the fast current conductances using the instantaneous approximation. This is equivalent to ignoring the detailed time dependences of all processes occurring on timescales of order several msec or less and instead considering them instantaneous. This assumption replaces the differential equation (2.1) with the simpler algebraic condition obtained by setting each side of (2.1) to zero

$$F(V) = -U + I. \tag{2.3}$$

Equation (2.2) remains unchanged. Corrections to the instantaneous approximation can be computed by what is known as singular perturbation theory [12].

By rescaling the time, replacing the current U and voltage V by appropriately shifted and scaled dimensionless variables u and v, and rescaling I we can rewrite the model as

$$f(v) = -u + I - \theta \tag{2.4}$$

and

$$\tau \frac{\mathrm{d}u}{\mathrm{d}t} = av - (1-a)u \tag{2.5}$$

with $f(v)$ given by

$$f(v) = \begin{cases} v - 2 & v \geq 1 \\ -v & -1 < v < 1 \\ v + 2 & v \leq -1. \end{cases} \tag{2.6}$$

The parameter θ corresponds to an offset current in the model while a provides, roughly speaking, a measure of the impact of the negative resistance region on the dynamics. Throughout, we will consider the range

$$\tfrac{1}{2} < a < 1. \tag{2.7}$$

For $0 < a < \frac{1}{2}$ the model can display bistable behaviour rather than oscillation which might have interesting applications as a latching mechanism [13], but this parameter range is not considered here.

Although the fast current has been specified for all v values, with certain restrictions the exact form of $f(v)$ for $-1 < v < 1$ is irrelevant to the behaviour of the model. This is because the model neuron will never spend any appreciable time in a state characterised by $-1 < v < 1$. Instead it will jump instantaneously (in a time of order 1 msec) between $v \leq -1$ and $v \geq 1$.

Note that $f(v)$ has a multivalued inverse. To deal with this problem it is convenient to introduce a binary variable S which denotes which branch of the function $f(v)$ is being used

$$S = \begin{cases} +1 & v \geq 1 \\ -1 & v \leq -1 \end{cases} \tag{2.8}$$

so that in the relevant regions $v \leq -1$ and $v \geq 1$ the rapid component of the membrane current can be written as

$$f(v) = v - 2S. \tag{2.9}$$

If the sign of S is flipped from $S = +1$ to $S = -1$ when v hits the boundary $v = 1$ of the upper branch of $f(v)$ and likewise is flipped from $S = -1$ to $S = +1$ when v passes through -1, this formula will always give the correct expression for $f(v)$. The condition (2.8) and this flipping can be implemented by requiring that

$$S = \mathrm{sgn}[S + I - \theta - u]. \tag{2.10}$$

It is interesting that in this approach the binary variable S arises as a label of the two branches of a function with a multivalued inverse. We can now solve (2.4) for v

$$v = I + 2S - \theta - u \tag{2.11}$$

and rewrite (2.5) as

$$\tau \frac{\mathrm{d}u}{\mathrm{d}t} = -u + a(I + 2S - \theta). \tag{2.12}$$

Equations (2.12) and (2.10) and the parameters a, θ and τ define the model. Although it is not directly an equation determining the dynamics of the model (2.11) is extremely useful since it gives the spike-averaged cell potential. As mentioned before, this can be used as a measure of the action potential spiking rate. The behaviour of the model can be determined simply by performing the appropriate integration of (2.12).

Thus far, the model has been described using the differential equation (2.12). However, if the model is run in discrete time steps of 1 unit (of order 1 msec) then the

dynamics can be given by two mapping rules, one which keeps track of which branch of $f(v)$ is being used by maintaining the correct value of S

$$S(t+1) = \mathrm{sgn}[S(t) + I(t) - \theta - u(t)] \tag{2.13}$$

and the other obtained by integrating (2.12) over one unit of time

$$u(t+1) = u(t)\mathrm{e}^{-1/\tau} + a(I(t) + 2S(t) - \theta)(1 - \mathrm{e}^{-1/\tau}). \tag{2.14}$$

The variable τ sets the timescale for all slow processes in the model. Clearly for $\tau \gg 1$ these discrete maps are identical to the original differential equation. Of course, in this case, we could replace the exponentials in (2.14) by linear approximations to them, but there is no real advantage in this. Provided that τ is bigger than about 5 of the time step units (about 5 msec) the behaviour of the model roughly scales in time with τ. In the simulations shown τ has been taken to be 50 although other values were tried to establish the appropriate scaling.

Note that for sufficiently large currents the factor I in (2.13) will overwhelm the factor $S - u$ and thus the model neuron reduces in this case to the Hopfield neuron of (1.7). For more moderate current values, however, the model exhibits a variety of dynamic effects reflecting the presence of the slow timescale.

The easiest way to visualise the behaviour of the model given by (2.10) and (2.12) is the method of isoclines shown in figure 1. In the uv plane we plot the curve $u = I - \theta - f(v)$ given by (2.10), and the set of points $u = av/(1-a)$ which make $\mathrm{d}u/\mathrm{d}t$ in (2.12) vanish. Throughout this paper, when a value for the parameter a is needed we will use $a = \frac{3}{4}$, a value midway in its allowed range. This has been done in figure 1, and in addition we have taken $I = \theta = 0$ in this figure. The dynamics of the model in the uv phase plane is such that motions affecting only v (horizontal motions) are rapid while any changes that modify the value of u are slow. Starting from an arbitrary point in the plane, the dynamics will immediately (in one time step) move the system to either the right ($v \geq 1$) or left ($v \leq -1$) linear branch of the curve $u = I - \theta - f(v)$ by changing the value of v, leaving u frozen near its initial value. Once u and v lie on the curve $u = I - \theta - f(v)$, they will slowly progress along it with both u and v changing their values. The motion will be toward the intersection of this curve with the line $u = av/(1-a)$. The timescale for this motion is τ. If during their motion along the curve $u = I - \theta - f(v)$ the variables u and v arrive at the point $v = -1$, $u = I - \theta - 1$, there will be an immediate jump to the right linear branch of this isocline caused by a sudden change in the value of v. A similar left jump will occur at the point $v = 1$, $u = I - \theta + 1$ when it is approached from the region $v > 1$. Although figure 1 is drawn with $I = \theta = 0$, the effect of non-zero I or θ can be visualised by moving the piecewise linear curve in figure 1 up or down by an amount $I - \theta$. By performing this shift the effect of a current pulse can be determined. Of course, when the model is on the right portion of the piecewise linear curve $S = +1$ and on the left $S = -1$.

To describe a system of N coupled neurons we let each model neuron have its own parameters a_i, θ_i and τ_i with $i = 1, \ldots, N$ and map from one time step to the next by

$$S_i(t+1) = \mathrm{sgn}[S_i(t) + I_i(t) - \theta_i - u_i(t)] \tag{2.15}$$

and

$$u_i(t+1) = u_i(t)\mathrm{e}^{-1/\tau_i} + a_i(I_i(t) + 2S_i(t) - \theta_i)(1 - \mathrm{e}^{-1/\tau_i}) \tag{2.16}$$

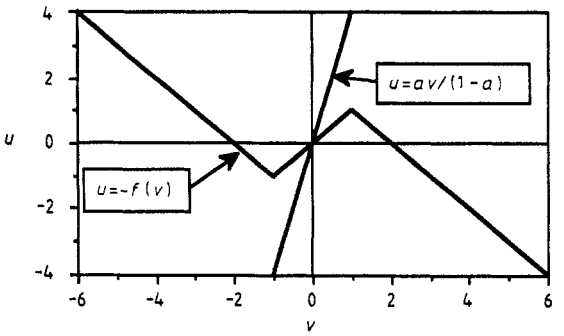

Figure 1. Isoclines corresponding to the model equations for one cell. The variable v will change rapidly until it lies somewhere on the curve $u = -f(v)$. Motion along this curve will be much slower and will always be toward the point where this curve meets the line $u = 3v$ (for $a = \frac{3}{4}$). When the corners at $v = \pm 1$ are reached v will suddenly change while u remains fixed. This jumps the system between the left and right branches of the piecewise linear curve. For non-zero I or θ the piecewise linear curve is shifted up or down by an amount $I - \theta$.

where, as in the Hopfield model,

$$I_i(t) = \sum_{j=1}^{N} J_{ij} S_j(t) + I_i^{\text{ext}}(t). \tag{2.17}$$

Once again in the limit of large couplings J_{ij} this model reduces to the ordinary Hopfield model. When we consider networks of model neurons we will take all a_i and θ_i to be the same (specifically, we will take $a_i = \frac{3}{4}$ and $\theta_i = 0$) and consider distributions of time constants τ_i. Of course, distributions over the variables a_i and θ_i could be considered as well.

Our goal is to analyse the behaviour of such a system and in particular its dependence on the coupling matrix J_{ij}, and the distribution of time constants τ_i. However, before doing this we will consider the behaviour of single model cells and pairs of coupled cells.

3. Single cell behaviour

The behaviour of a single model neuron is given by (2.13) and (2.14) which can be analysed with the aid of figure 1. In the presence of a constant current (including zero current), the cell will remain in a passive state, $S = -1$, if

$$I - \theta \leq -\frac{2a - 1}{1 - a}. \tag{3.1}$$

It will remain in an active, firing state, $S = +1$, if

$$I - \theta \geq \frac{2a - 1}{1 - a} \tag{3.2}$$

and it will oscillate between the $S = +1$ and $S = -1$ states if

$$-\frac{2a - 1}{1 - a} < I - \theta < \frac{2a - 1}{1 - a}. \tag{3.3}$$

In the case of oscillation, the cell will remaining in the $S = +1$ state for a period of time

$$T_+ = \tau \ln \left[\frac{2a + 1 - (1-a)(I-\theta)}{2a - 1 - (1-a)(I-\theta)} \right] \tag{3.4}$$

and in the state $S = -1$ for a time

$$T_- = \tau \ln \left[\frac{2a + 1 + (1-a)(I-\theta)}{2a - 1 + (1-a)(I-\theta)} \right]. \tag{3.5}$$

These formulae indicate that the behaviour of a cell in the absence of external or synaptic currents can be controlled, for example, by adjusting the parameter θ. For fixed values of parameters, cell behaviour can be modified by external or synaptic currents. In these ways the cell can be placed in a passive, active or oscillating state with the period and the ratio of on ($S = +1$) to off ($S = -1$) times fully adjustable either by changing the parameters of the model or through external or synaptic currents.

The variety of behaviours exhibited by a single model neuron is shown in figure 2. In figure 2(a), the response of a cell which is normally passive ($a = \frac{3}{4}$ and $\theta = 3$) to external current pulses I is shown. Such a passive model cell has a resting potential

$$v_R = -(1-a)(\theta + 2). \tag{3.6}$$

To become excited to the $S = +1$ state, the potential v must be pushed above -1 which is possible if the model cell is exposed to a positive current pulse of amplitude A satisfying

$$A > 1 - 2a + (1-a)\theta. \tag{3.7}$$

A short current pulse of this amplitude will temporarily raise v to an excited level $v = 4 - (1-a)(\theta + 2) > 1$ and the cell will remain in the $S = +1$ state until v goes down to 1 at which point it will return to the $S = -1$ state. The time for this to happen and thus the duration of the plateau can be computed directly

$$T_{\text{plateau}} = \tau \ln \left[\frac{4a}{(2a-1) + (1-a)\theta} \right] \tag{3.8}$$

and it can be significantly longer than the duration of the current pulse itself. This plateau property is demonstrated by the first current pulse and response shown in figure 2(a).

We have seen that it takes a positive current of magnitude $A > 1 - 2a + (1-a)\theta$ to excite a normally passive cell to the active state. However, immediately after a plateau burst, the cell is in a hyperpolarised state $u = 1 - \theta$, $v = -3$. At this time, a current pulse of magnitude $A > 2$ is required to re-excite the cell. If $\theta < (2a + 1)/(1 - a)$ this current is greater than the current need to excite the cell from its resting potential and the model exhibits postfiring inhibition.

The second current applied in figure 2(a) is a short negative pulse that causes a reduction of v but no change in the state $S = -1$ of the cell. However, a longer pulse applied after that induces a postinhibitory rebound. To induce a rebound from the

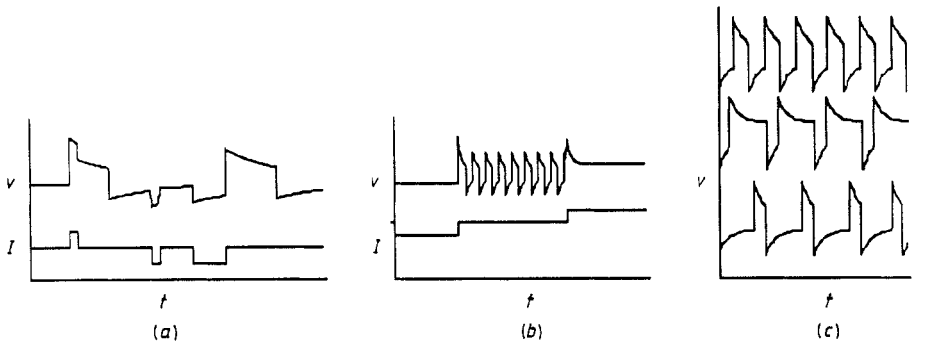

Figure 2. The behaviour of a single model cell. (*a*) shows the response of a cell to various current pulses. First a positive current pulse induces a plateau lasting much longer than the current pulse itself. Next a negative current pulse of short duration produces no lasting change in the state of the cell. However, a subsequent longer pulse causes a post-inhibitory rebound to another plateau. (*b*) shows how a negative constant current can freeze a cell into the $S = -1$ state while it oscillates in the absence of current and freezes into the $S = +1$ state when a postive current is applied. In (*c*) various oscillatory waveforms obtained by varying the parameter θ are illustrated.

$S = -1$ state to $S = +1$, the variable u must be reduced to $u < -1 - \theta$. This requires a negative current pulse of magnitude A satisfying

$$A > \frac{1 - 2a + (1 - a)\theta}{a}. \tag{3.9}$$

In addition it takes a time

$$T_{\text{pulse}} > \tau \ln \left[\frac{aA}{2a - 1 - (1 - a)\theta + aA} \right] \tag{3.10}$$

for u to be reduced to this value. Both of the above conditions must be met for a pulse to induce the rebound phenomenon. If a long pulse of sufficient magnitude A is applied the duration of the $S = +1$ rebound will be

$$T_{\text{rebound}} = \tau \ln \left[\frac{a(A + 4)}{2a - 1 + (1 - a)\theta} \right]. \tag{3.11}$$

Note that the more negative the current pulse is (i.e. the large its magnitude A) the longer the rebound plateau lasts.

Figure 2(*b*) shows an oscillating cell ($a = \frac{3}{4}$ and $\theta = 0$) in the presence of three constant currents. First, a negative current freezes the model cell into the $S = -1$ state. Then, under zero current the cell oscillates, and finally with a positive I the cell is held in the $S = +1$ state. This property allows other cells to modulate the behaviour of the model cell through synaptic couplings. In figure 2(*c*) various oscillatory waveforms obtained by varying θ with $I = 0$ are shown. The oscillation may be symmetric or either predominantly $S = +1$ or predominantly $S = -1$. This variety of behaviours could also be induced by non-zero external currents which, up to a sign, have the same effect as a shift in the value of the parameter θ. All of the results related to figure 2 can be obtained analytically from the model equations. The simulation used to generate this figure is just a realisation of the iterations (2.13) and (2.14).

4. Two coupled cells

Before considering a network of cells, two interesting behaviours displayed by a pair of coupled model cells will be illustrated. A coupled pair of identical van der Pol oscillators has been considered in the original differential equation form elsewhere [14]. Here, I will concentrate on two cases for which one or both of the cells is not an intrinsic oscillator.

Consider first a pair of passive cells coupled by mutually inhibitory couplings, an arrangement known as a half-centred oscillator. If the coupling is strong enough so that the bound (3.9) is satisfied by the inhibitory synaptic current, and if the duration of the induced rebound plateau in one cell (3.11) is longer than the length of the pulse (3.10) needed to induce post-inhibitory rebound in the other cell, sustained oscillations can be realised. This is shown in figure 3(*a*). The oscillations are started by placing one cell in the excited $S = +1$ state and the other in the passive $S = -1$ state. When the $S = +1$ plateau of the excited cell terminates, the release from inhibition causes the second cell to jump to the $S = +1$ state until its plateau terminates. The process continues like this indefinitely despite the fact that neither cell has any intrinsic oscillatory properties, nor are any positive synaptic currents present which could induce oscillation in either cell separately.

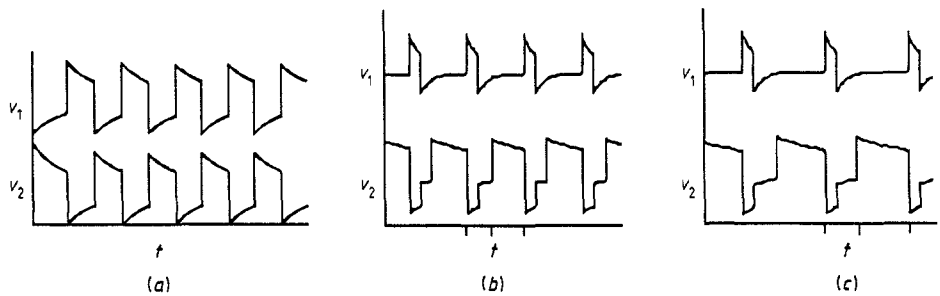

Figure 3. The behaviour of two coupled model cells. In (*a*) two normally silent cells are coupled with mutual inhibition. Starting with one cell in the $S = +1$ state, the plateau behaviour and postinhibitory rebound produce stable oscillations. (*b*) and (*c*) show an oscillatory cell coupled with inhibitory coupling to a tonically active cell with a very slow time constant. In this case, the slow cell acts as a fixed-phase follower, firing at a fixed phase angle during the cycle of the oscillator independent of the oscillatory frequency. This is shown for two frequencies in (*b*) and (*c*), where the frequency of the oscillator has been adjusted without changing any of the parameters governing the follower cell.

A second interesting example occurs when an oscillatory cell interacts with another cell which would remain continually in the state $S = +1$ in the absence of coupling. The only interaction between the two cells is an inhibitory synaptic coupling from the oscillator to the tonically active cell. For simplicity we assume that the oscillator produces a short burst of activity during its cycle. In addition, the intrinsic time constant of the active, non-oscillatory cell is taken to be much longer than the period of the oscillator. In this case the slow, active cell will act as a fixed-phase follower.

The activity of this pair of cells is shown in figure 3(*b*) and 3(*c*). Let us begin the analysis of the situation at the time during the cycle when cell 2 (the follower or non-oscillatory cell) first goes to the active $S = +1$ state. At this moment $u = -1 - \theta$

for the follower cell. The variable u will grow from this value until the active period is terminated by the inhibitory pulse from the oscillator, cell 1. If this active state lasted for a time t_{on} then at this point u will be given by

$$u_f = -(1+\theta)e^{-t_{on}/\tau} + a(2-\theta)(1-e^{-t_{on}/\tau}) \tag{4.1}$$

where a, θ and τ refer to the parameters of the follower (those of the oscillator will not enter the discussion). When cell two is in the $S = -1$ state, u decreases from this value until it reaches $-1-\theta$ and the follower becomes excited again completing one cycle. This re-excitation will take a time

$$t_{off} = \tau \ln\left[\frac{u_f + a(2+\theta)}{a(2+\theta) - 1 - \theta}\right]. \tag{4.2}$$

If, as we have assumed, $\tau >> t_{on}$ and $\tau >> t_{off}$ we can expand these expressions to get a simple relation between t_{off} and t_{on}, namely

$$t_{off} = \left(\frac{2a+1+(1-a)\theta}{2a-1-(1-a)\theta}\right) t_{on}. \tag{4.3}$$

The phase during the cycle when cell 2 begins to fire is given by

$$\phi = \frac{t_{off}}{t_{off}+t_{on}} = \frac{2a+1+(1-a)\theta}{4a}. \tag{4.4}$$

The key feature of this result is that it depends only on the parameters associated with the follower cell and in particular is independent of the frequency and waveform of the oscillatory pacemaker. This means that the firing of the slow follower cell will follow that of the fast pacemaker with a time delay which varies in precisely the right way to maintain a constant phase difference no matter what the frequency of the cycle is.

The fixed-phase of the follower can be seen by comparing figure 3(b) with figure 3(c) where the behaviour of the two cells is shown for two different cycle frequencies. These figures have been obtained by changing the behaviour of the oscillator without adjusting the parameters of the follower cell in any way. The fixed-phase behaviour of the follower is an automatic dynamical adjustment. This feature provides an extremely valuable tool for constructing network generators which can produce a fixed pattern of activity over a wide range of frequency. For example, a chain of such follower cells driven at one end by an oscillator can provide a travelling wave with fixed phase shift per segment over a wide range of driving frequencies. However, it should be noted that the oscillator follower arrangement is only stable for

$$\phi < \tfrac{1}{2}. \tag{4.5}$$

Thus, for the fixed phase follower to work we must require

$$-\frac{2a+1}{1-a} < \theta < -\frac{1}{1-a}. \tag{4.6}$$

The bound of $\frac{1}{2}$ on the fixed phase ϕ is true for any follower like the one being discussed which has the property that the time spent in the silent state during one

cycle is proportional to the time spend firing in the previous cycle. If we number the cycles using the label n then

$$t_{\text{off}}^{(n)} = \alpha t_{\text{on}}^{(n-1)} \tag{4.7}$$

where for the present case

$$\alpha = \frac{2a + 1 + (1-a)\theta}{2a - 1 - (1-a)\theta} \tag{4.8}$$

and the fixed phase angle is

$$\phi = \frac{t_{\text{off}}}{t_{\text{off}} + t_{\text{on}}} = \frac{\alpha}{1+\alpha} = \frac{2a + 1 + (1-a)\theta}{4a}. \tag{4.9}$$

To solve the recursion relation (4.7) we note that $t_{\text{off}} + t_{\text{on}}$ is just the total period of the driving oscillator T. The fixed-point solution of (4.7) is then

$$t_{\text{off}} = \frac{\alpha T}{1+\alpha} \qquad t_{\text{on}} = \frac{T}{1+\alpha}. \tag{4.10}$$

The stability of this fixed point can be tested by writing

$$t_{\text{off}}^{(n)} = \frac{\alpha T}{1+\alpha} + \delta_n \tag{4.11}$$

and

$$t_{\text{on}}^{(n)} = \frac{T}{1+\alpha} - \delta_n. \tag{4.12}$$

Then (4.7) turns into a simple recursion relation for δ_n

$$\delta_n = -\alpha \delta_{n-1}. \tag{4.13}$$

This shows immediately that the fixed-point solution is only stable for $\alpha < 1$ or, equivalently, $\phi < \frac{1}{2}$.

5. Response of a single cell to an oscillating current

In the next section we will consider the phase locking of a large system of coupled model oscillators. We will find that for certain parameter ranges synchronous phase locking occurs with the entire network of oscillators acting in unison. The effect of this on any one oscillator of the network is to produce a synaptic current which is a square wave. Therefore, a mean-field approximation for the behaviour of a set of coupled oscillators is provided by studying a single oscillator being driven by an external square-wave current. Driven van der Pol oscillators have been treated previously [15] and our results are similar to these numeric results, but for this simplified model we will obtain analytic conditions for the phase locking of the driven cell which can be used as the basis of a mean-field description of the oscillatory network.

Consider a single oscillator described by (2.13) and (2.14) where for simplicity we will take $\theta = 0$ corresponding to a symmetric intrinsic oscillator. We drive this oscillator with an external current consisting of a square wave oscillating between $I = \pm A$ with a period T. Figure 4 shows a plot of the variable u of the driven cell measured at integer multiples of the driving period for a wide range of driving periods. For this plot the amplitude of the driving current was taken to be $A = 0.25$ and at each value of T the cell was run for 50 cycles to relax the oscillator and then 100 points were plotted. Shown in the figure are regions of chaotic behaviour, various cycles and a window of phase locking around $T = T_0$ where T_0 is the intrinsic period of the oscillator. It is this phase-locking window which will be of interest for network application.

The boundaries of the phase-locking window can be calculated analytically. For a driving force faster than the natural period of the oscillator,

$$T_0 = 2\tau \ln\left[\frac{2a+1}{2a-1}\right] \tag{5.1}$$

the critical condition is that u must go from the value $A-1$ to the value $1-A$ during the time that the current takes the value $I = A$, a time $T/2$. When driven slower than its natural period, the oscillator must go from $u = -1-A$ to $u = 1-A$ while the current has the value $I = -A$ and then go from $u = 1-A$ to $u = 1+A$ while the current is $I = A$ all in one half the driving period, $T/2$. From this we find that phase-locking will occur in the range

$$2\tau \ln\left[\frac{2a+1-(1-a)A}{2a-1+(1+a)A}\right] < T < 2\tau \ln\left[\frac{(1-a^2)A^2+6aA+4a^2-1}{(2a-1)^2-(a-1)^2A^2}\right]. \tag{5.2}$$

In the region indicated by the steeply falling curve in figure 4, the driven cell follows the driving current but is not synchronous with it. The critical condition for synchronous phase locking when the oscillator is driven more slowly than its natural period, is that it must go from $u = -1-A$ to $u = 1+A$ while $I = A$ in a time $T/2$. Therefore, synchronous phase-locking occurs only in the more restricted region

$$2\tau \ln\left[\frac{2a+1-(1-a)A}{2a-1+(1+a)A}\right] < T < 2\tau \ln\left[\frac{2a+1+(1+a)A}{2a-1-(1-a)A}\right]. \tag{5.3}$$

These results are summarised in figure 5 (for $a = \frac{3}{4}$) which will provide a basis for the analysis of a network of oscillators. The lower bound for locking goes to zero at a current magnitude $A = 1$ because for this value the cell can remain at the fixed value $u = 0$ while v jumps back and forth regardless of how fast the driving current oscillates. The upper bound for phase locking goes to infinity when $A = (2a-1)/(1-a)$ which is the point at which the cell will follow the current no matter how slow it goes because intrinsic oscillation has been halted by the imposed current.

6. A network of oscillators

Phase locking is a well known phenomenon [16] exhibited by systems of coupled oscillators so it should be no surprise that a network of model oscillators can display this effect. What is exceptional about the present model is that phase locking can be

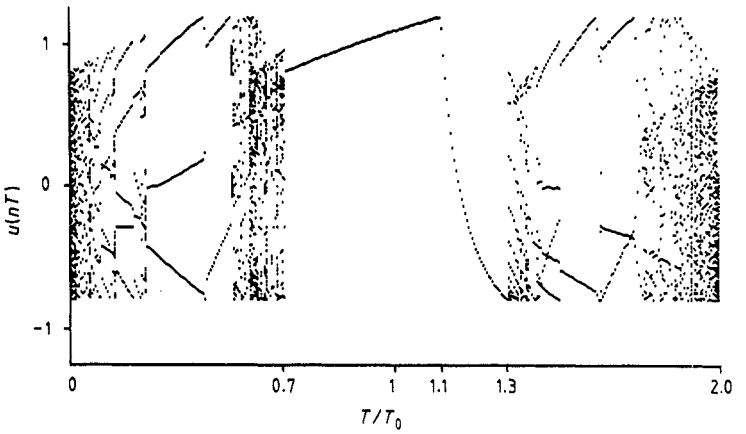

Figure 4. A single model cell driven by an external square wave. The slow current u has been plotted at integer multiples nT of the driving period T for $n = 50 \ldots 150$. T_0 is the intrinsic period of the cell. A region of phase locking in the neighbourhood of $T = T_0$ can be seen. For this figure the amplitude of the driving square wave was 0.25 and $\theta = 0$ with $a = \frac{3}{4}$.

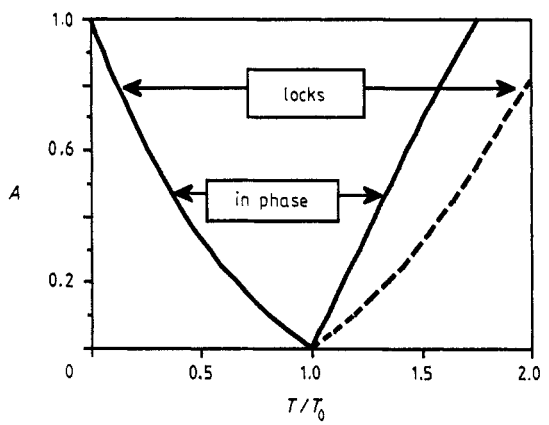

Figure 5. The behaviour of a driven model cell. T is the driving period, T_0 the intrinsic period of the oscillatory cell and A the amplitude of the driving square wave. Between the full curves synchronous phase locking occurs. Inside the broken line is a region where the cell locks but is out of phase with the driving current. Outside these lines no phase locking occurs.

treated analytically (although fairly crudely) even for strong coupling while keeping the full nonlinearity of the underlying oscillators intact. After treating the problem in mean-field theory we will compare the results with those that are obtained using a phase-coupling approximation for the network of oscillators.

We will consider at first a uniform coupling of N oscillators described by (2.15), (2.16) and (2.17) with the coupling matrix

$$J_{ij} = \frac{A}{N-1}(1 - \delta_{ij}). \tag{6.1}$$

When the network is in the state $S_i = +1$ (for all i) each cell receives a synaptic current $I_i = A$ while in the state $S_i = -1$ the synaptic current is $I_i = -A$. For

the individual oscillators we will take $a_i = \frac{3}{4}$, $\theta_i = 0$, but the time constants τ_i will be chosen randomly over a specified range. Since all the network cells are intrinsic oscillators we can equivalently choose their natural periods randomly and uniformly over a range

$$T_{\min} \leq T_0 < T_{\max}. \tag{6.2}$$

We can characterise the behaviour of such a network using the alignment of the state S_i at time t

$$m(t) = \frac{1}{N}\sum_{i=1}^{N} S_i \tag{6.3}$$

to characterise the system. We denote time averages by angle brackets. For example, $\langle m \rangle$ is the value of $m(t)$ averaged over a long period of time starting after the system has relaxed. Three types of behaviour are observed. For small coupling A, the cells all oscillate independently so $\langle m \rangle = \langle m^2 \rangle = 0$. For larger coupling the oscillators phase lock and the whole network oscillates between the states $S_i = +1$ and $S_i = -1$. In this case, the average value of m is zero, since the system oscillates symmetrically between $m = +1$ and $m = -1$. Phase locking is signalled by a non-zero value of $\langle m^2 \rangle$ so that $\langle m \rangle = 0$ while $\langle m^2 \rangle \neq 0$. Finally, for $A \geq 2$, the model neuron becomes equivalent to a Hopfield neuron and the model just described goes over to the infinite range Ising model. At the point $A = 2$, there is a sudden transition from a state characterised by $\langle m \rangle = 0$ and $\langle m^2 \rangle = 1$ to a state with $\langle m \rangle = \pm 1$ and $\langle m^2 \rangle = 1$ and the phase-locked oscillating state turns into a frozen, aligned ferromagnetic state.

When phase-locking occurs, all sites i make the transition $S \rightarrow -S$ at virtually the same moment. Thus, the synaptic input to each cell looks like a square wave of amplitude A. The mean-field approximation consists of demanding that each individual cell be capable of phase-locking with this square wave input. For this situation, we are only interested in the synchronous phase locking region. We will assume that the lower limit of (5.3) for $T_{\min}$ and the upper limit for $T_{\max}$ can be used to determine the ratio of the maximum to minimum periods allowed. We find that for a given coupling strength A, locking should occur if

$$\frac{T_{\max} - T_{\min}}{T_{\max} + T_{\min}} \leq \ln\left[\frac{(10+7A)(2+7A)}{(2-A)(10-A)}\right]\left\{\ln\left[\frac{(10+7A)(10-A)}{(2-A)(2+7A)}\right]\right\}^{-1}. \tag{6.4}$$

To keep this equation manageable the value $a = \frac{3}{4}$ has been substituted in. This mean-field result is quite crude in that it does not depend on the exact form of the probability distribution governing individual oscillator frequencies. Instead it only depend on the boundaries of this distribution. We expect that effects of different distributions only modify our results by a factor of order one, at least for distributions with definite boundaries.

The result (6.4) has the great advantage of being applicable even for large differences in intrinsic periods, $(T_{\max} - T_{\min})/(T_{\max} + T_{\min})$ near one, and strong coupling, A of order one. For a given ratio $(T_{\max} - T_{\min})/(T_{\max} + T_{\min})$ we define the critical value of A as the minimum value which allows for phase-locking. The value of this A_c from (6.4) is plotted against $(T_{\max} - T_{\min})/(T_{\max} + T_{\min})$ in figure 6. Also shown in this figure is data taken from computer simulation of the model with both $N = 50$ and

$N = 100$. The simulation was done by starting the system in the state $S_i = 1$ with u_i chosen randomly between -1 and $+1$. For given values of T_{max} and T_{min} the individual time constants τ_i were chosen randomly and uniformly in the appropriate range. After an initial relaxation period, $m(t)$ was computed at each time step, squared and averaged over many subsequent time steps. The simulation was repeated using several different random choices of intrinsic periods and starting u values. From these results the critical value of A was determined by defining the transition to a phase-locked state as occurring somewhere in the range between $\langle m^2 \rangle$ of 0.4 and 0.6. The data shown in figure 6 indicate excellent agreement with the mean-field result for this case.

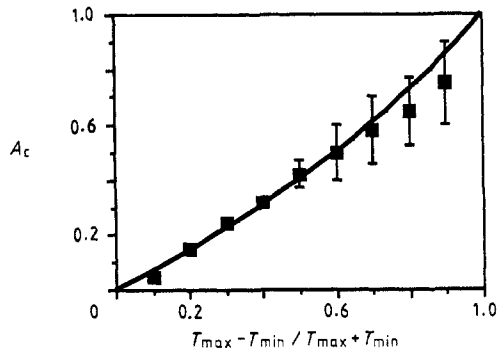

Figure 6. The predicted critical coupling A_c for a network of oscillators as a function of the range of intrinsic oscillator periods. The predicted curve is obtained from results on a single driven cell. The data points are from repeated simulations with networks of 50 and 100 cells.

A common method for analysing systems of oscillators is the phase-coupling approximation [16, 17]. This consists of describing each oscillator in terms of a phase variable $\phi_i(t)$ which changes by 2π during the course of an oscillatory cycle. The phase is defined so that it evolves linearly with time, $\phi_i(t) = \phi_i(0) + \omega_i t$ in the absence of coupling. The coupling is then modelled by an effective interaction involving only the difference in the phases of the coupled oscillators. Since the ferromagnetic coupling we have used thus far tends to bring two coupled oscillators into phase with each other, we write the coupled system as

$$\frac{d\phi_i}{dt} = \omega_i + \frac{\tilde{A}}{N} \sum_{j=1}^{N} \sin[\phi_j - \phi_i]. \tag{6.5}$$

The coupling parameter $\tilde{A}$ is a renormalised effective coupling strength. It is presumably proportional to A, at least for small coupling. On dimensional grounds we take

$$\tilde{A} \propto \frac{A}{T_{max} + T_{min}}. \tag{6.6}$$

Note that the phase-coupling model is quite different in structure from the original model. In fact for many purposes it does not provide an adequate description. However, in certain cases it may give some reliable results [17].

The system of phase equations (6.5) has been considered in great detail [16]. For this system the critical coupling strength for phase locking is given by

$$\tilde{A}_c \propto \frac{T_{max} - T_{min}}{T_{max} T_{min}}. \tag{6.7}$$

The constant of proportionality can be computed but will not be need for our purposes. Instead, this constant and the unknown constant in (6.6) can be determined by comparing this result with the value of A_c given by figure 6. A good fit for small couplings is given by

$$A_c = \frac{0.17(T_{max} - T_{min})(T_{max} + T_{min})}{T_{max} T_{min}}. \tag{6.8}$$

This result agrees with the mean-field result when T_{max} and T_{min} are close to each other and A_c is small. However, as $(T_{max} - T_{min})/(T_{max} + T_{min}) \to 1$ the phase-coupling approximation predicts $A_c \to \infty$ when in fact $A_c \to 1$ in this limit. This is because the phase-coupling model does not contain any information about the fact that these oscillators can be frozen by large enough currents. Nevertheless, up to about $(T_{max} - T_{min})/(T_{max} + T_{min}) = 0.5$ the phase-coupling result is quite accurate. In this region the difference between the phase-coupling and mean field results is at most about 10%. Actually, if a simple analytic expression for the curve in figure 6 is desired the result

$$A_c \approx \frac{0.8(T_{max} - T_{min})}{T_{max} + T_{min}} \tag{6.9}$$

provides a much better fit.

7. An oscillator associative memory

When $\theta_i = 0$, the cell model given by (2.13), (2.14) and (2.17) has a local invariance

$$S_i \to \xi_i S_i \qquad u_i \to \xi_i u_i \qquad J_{ij} \to J_{ij} \xi_i \xi_j \tag{7.1}$$

for an arbitrary pattern $\xi_i = \pm 1$. Because of this, we could have evaluated phase locking of the state $S_i = \pm \xi_i$ using the coupling matrix

$$J_{ij} = \frac{A}{N-1} \xi_i \xi_j (1 - \delta_{ij}) \tag{7.2}$$

in the last section and we would have obtained identical results. This raises the possibility of phase locking into one of a number of different target patterns $\xi_i^\mu = \pm 1$ for $\mu = 1, \ldots, P$. The easiest way to do this is to use the Hebb matrix [18]

$$J_{ij} = \frac{A}{N-1} \sum_{\mu=1}^{P} \xi_i^\mu \xi_j^\mu (1 - \delta_{ij}). \tag{7.3}$$

It has been shown that for the Hopfield model, an initial state near $S_i = \xi_i^\mu$ for some μ value will reach a final state with overlap

$$m = \frac{1}{N}\sum_{i=1}^{N} \xi_i^\mu S_i \tag{7.4}$$

very near 1 provided that $P < 0.14N$ [19]. Here something very similar happens. Figure 7(*a*) shows the time dependent value of m with ξ_i^μ chosen randomly from $P = 10$ memory patterns in an $N = 100$ network ($\alpha = P/N = 0.1$). In this case the initial state was chosen to be $S_i = \xi_i^\mu$ with the initial u_i chosen randomly. The random, uniformly distributed range of natural frequencies for the oscillators was $(T_{\max} - T_{\min})/(T_{\max} + T_{\min}) = 1/2$ and the coupling strength was take to be $A = 1$. As can be seen, m oscillates between $+1$ and -1 indicating phase locking onto this memory pattern. The network is similarly able to phase lock onto any one of the ten stored patterns. On the other hand if the memory is overloaded as in figure 7(*b*) where $P = 20$ patterns have been encoded into a Hebb matrix for $N = 100$, no memory phase locking is evident.

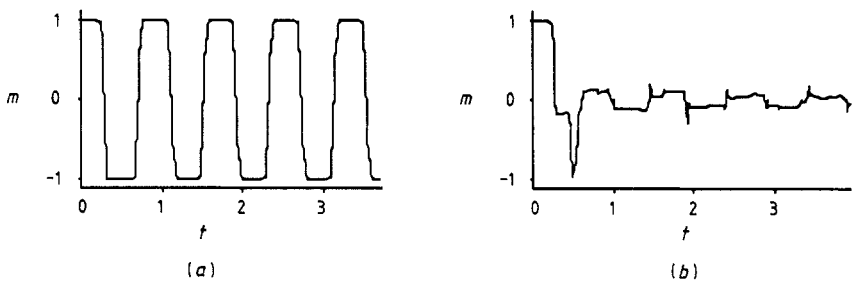

Figure 7. The overlap m of an oscillatory associative memory with one of the stored memory patterns as a function of time. In (*a*) 10 patterns are stored in a 100 x 100 Hebb matrix and memory recovery is indicated by phase locking. When storage of 20 patterns is attempted, no phase locking occurs (*b*).

The storage capacity of such a phase-locking memory with Hebbian coupling is investigated in figure 8 for $N = 100$, $(T_{\max} - T_{\min})/(T_{\max} + T_{\min}) = 1/2$ and $A = 1$. We see that the storage capacity is approximately the same as that of the Hopfield model although some degradation of the recover is seen near $P = 10$. These data points represent the average of many runs with different random choices of memory patterns. Detailed examination reveals large fluctuations in performance for the region near $P = 10$ depending on the random choice of patterns.

There is clearly a minimum value of the coupling strength needed to obtain phase locking with a given number of stored memories as can be seen from figure 9. In addition, there is a maximum value of the coupling beyond which there is a transition to fixed-point rather than oscillatory behaviour. Both the minimum and maximum values can be estimated from the results of the last section and a knowledge of the properties of the synaptic current. For phase locking to occur without fixed point behaviour we must have

$$A_c < \sum_{j=1}^{N} J_{ij}\xi_i^\mu \xi_j^\mu < \frac{2a-1}{1-a}. \tag{7.5}$$

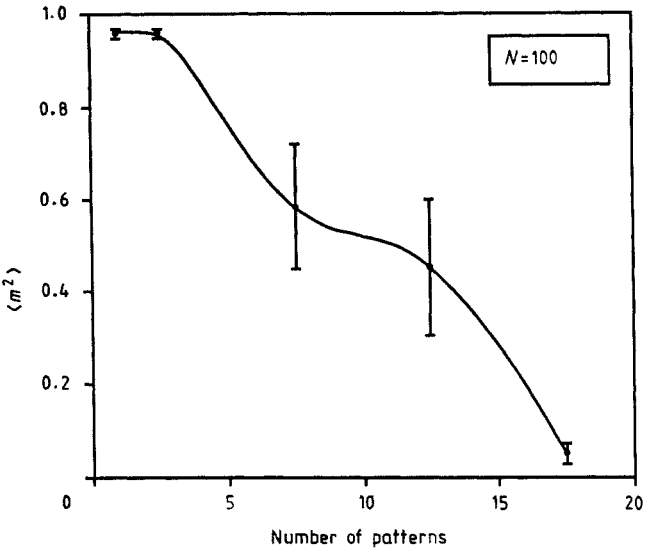

Figure 8. The time average of the square of the overlap with one memory pattern as a function of the number of patterns stored in an $N = 100$ network. The storage capacity is essentially the same as for a Hopfield network.

The critical coupling A_c is determined for given a, T_{max} and T_{min} by setting the upper and lower bounds of (5.3) to T_{max} and T_{min} respectively. For $a = \frac{3}{4}$, A_c is given by figure 6 or approximately by (6.9). Let us write the normalisation of the coupling matrix as

$$A_i = \left(\sum_{j=1}^{N} J_{ij}^2 \right)^{1/2} \tag{7.6}$$

and define

$$\gamma_i^\mu = \sum_{j=1}^{N} J_{ij} \xi_i^\mu \xi_j^\mu \left(\sum_{j=1}^{N} J_{ij}^2 \right)^{-1/2} . \tag{7.7}$$

Then, the condition for phase locking on the memory pattern ξ_i^μ can be written as

$$A_c < A_i \gamma_i^\mu < \frac{2a-1}{1-a} . \tag{7.8}$$

The reason for writing the condition (7.8) for phase locking in this form is that a great deal is known about the distribution of γ_i^μ values for particular forms of the coupling matrix. For example, a slight generalisation of the Hebb matrix (7.3)

$$J_{ij} = \frac{A_i}{\sqrt{P(N-1)}} \sum_{\mu=1}^{P} \xi_i^\mu \xi_j^\mu (1 - \delta_{ij}) \tag{7.9}$$

has the normalisation (7.6) and a γ_i^μ distribution which is Gaussian with unit width and mean value $\sqrt{N/P}$. Therefore, for the Hebb matrix we can substitute $\gamma_i^\mu =$

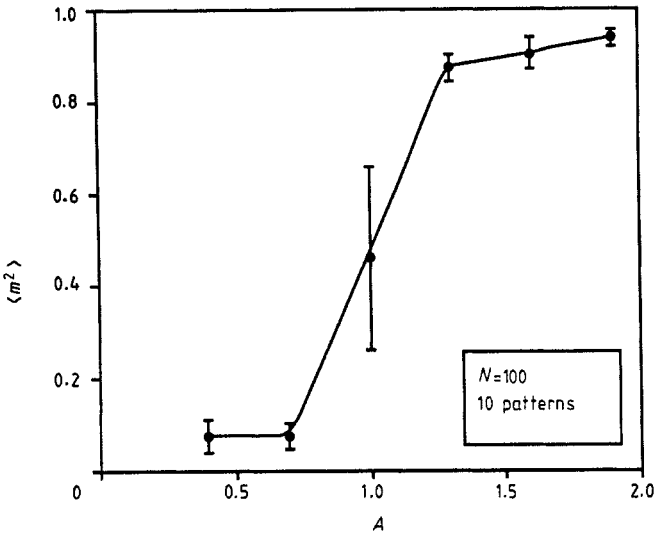

Figure 9. The time average of the square of the overlap for one memory state in a 100 node network storing 10 patterns. A is the magnitude of the coupling matrix. A value of $A > 1$ is needed for memory recall.

$\sqrt{N/P}$ in (7.8) to determine the condition on the A_i required for phase locking with oscillation.

Another commonly used form of the coupling matrix is the pseudoinverse [20]

$$J_{ij} = \frac{A_i}{\sqrt{PN - P^2}} \sum_{\mu,\nu}^{P} C_{\mu\nu}^{-1} \xi_i^\mu \xi_j^\nu (1 - \delta_{ij}) \tag{7.10}$$

where

$$C_{\mu\nu} = \frac{1}{N} \sum_{i=1}^{N} \xi_i^\mu \xi_i^\nu . \tag{7.11}$$

For the pseudoinverse matrix the γ_i^μ values are

$$\gamma_i^\mu = \sqrt{\frac{N - P}{P}} . \tag{7.12}$$

Substituting this into (7.8) gives the phase locking oscillation condition for the pseudoinverse matrix. The capacity of the oscillator memory is limited to $P < N$ just as in the non-oscillatory case.

Finally there is a well known class of coupling matrices satisfying [21, 22]

$$\gamma_i^\mu > \kappa . \tag{7.13}$$

These have a maximum storage capacity given by [22]

$$\alpha_{\max} = \left[\int_{-\kappa}^{\infty} \frac{dz}{\sqrt{2\pi}} e^{-z^2/2} (\kappa + z)^2 \right]^{-1} . \tag{7.14}$$

Near this memory saturation point the values of γ_i^μ accumulate near $\gamma_i^\mu = \kappa$ so in this case, phase locking will occur when (7.8) is satisfied with $\gamma_i^\mu = \kappa$.

The oscillatory associative memory can also be analysed using the phase-coupling approximation introduced in the last section. In this formalism the set of N oscillators is described N phase angles obeying the set of equations

$$\frac{\mathrm{d}\phi_i}{\mathrm{d}t} = \omega_i + \sum_{j=1}^{N} \tilde{J}_{ij} \sin[\phi_j - \phi_i] \tag{7.15}$$

where $\tilde{J}_{ij}$ is a renormalised coupling matrix and is assumed to be proportional to J_{ij}. The intrinsic frequencies ω_i are chosen from some probability distribution to be specified. For memory recovery we look for solutions of the form

$$\phi_i = \overline{\omega}\, t + \frac{\pi}{2}\xi_i^\mu + \epsilon_i \tag{7.16}$$

with $-\pi/2 < \epsilon < \pi/2$. The pattern $\xi_i^\mu = \pm 1$ which is one of the P patterns encoded in the coupling matrix $\tilde{J}_{ij}$ now appears as a measure of the phase of a particular oscillator. Note that

$$\sin[\phi_j - \phi_i] \approx \xi_i^\mu \xi_j^\mu \sin[\epsilon_j - \epsilon_i]. \tag{7.17}$$

Then, from (7.15) we find

$$\frac{\mathrm{d}\epsilon_i}{\mathrm{d}t} = \omega_i - \overline{\omega} + \sum_{j=1}^{N} \tilde{J}_{ij} \xi_i^\mu \xi_j^\mu \sin[\epsilon_j - \epsilon_i]. \tag{7.18}$$

This set of equations is currently being analysed. Although the phase-coupled model has some features in common with the model discussed in this paper and displays interesting dynamics, the above equations do not appear to provide an adequate description of the behaviour of the full model.

8. Discussion

Some of the behaviours seen in the network of oscillators we have been discussing are shown in figure 10. In figure 10(a) an uncoupled set of 50 oscillators with a variety of intrinsic frequencies is shown oscillating in a completely incoherent pattern. In figure 10(b) a coupling matrix which stores the pattern $\xi_i = +1$ has been applied and we see that phase locked oscillations between this pattern and its inverse occur. By adjusting the coupling strength at individual sites it is possible to get a subset of the oscillators to phase lock and oscillate between a given pattern and its inverse while freezing other sites in a fixed state. By doing this, we can get the network to oscillate coherently between any two patterns which are not necessarily inverses of each other as shown in figure 10(c).

In order to account in a more quantitative way for a variety of cell behaviours, more flexibility can be built into the model we have discussed in several ways. First the timescale τ can be made state dependent

$$\tau = \overline{\tau} + S\Delta\tau \tag{8.1}$$

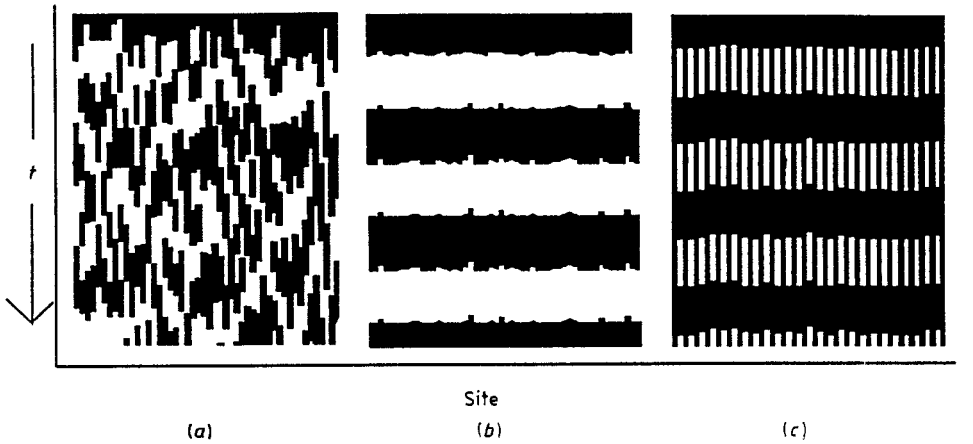

Figure 10. Three behaviours in a network of oscillators. Along the vertical axis time runs downward. The horizontal axis shows the i value of the cell being plotted. Black denotes the state $S = +1$ and white the state $S = -1$. The oscillators in (a) are uncoupled and oscillate incoherently. In (b) a coupling matrix storing the pattern $\xi_i^\mu = 1$ with sufficient strength induces phase locking. With a different form for the coupling matrix, the network can oscillate coherently between any two patterns as shown in (c).

so that the excited and silent state can be characterised by different intrinsic timescales. This has proven especially useful for constructing model pattern generators [23]. A tremendous variety of behaviours can be obtained by using different forms for the fast current $f(v)$. In biological cells, the excited state voltage region is usually characterised by a lower resistance than what is measured at lower voltages. More complicated shapes for $f(v)$ can give rise to delayed responses and more gradual changes of oscillator frequency with applied current.

It is clear that the slow timescale features discussed here play a vital role in central pattern generators [5]. Oscillatory and plateau cells are essential elements in biological central pattern generators and they cannot be replaced by simple instantaneous binary cells in any model which hopes to be at all realisitic. On the other hand, the model discussed here is ideally suited for simulations of the behaviour and dynamics of central pattern generators [23]. The fixed-phase follower analysed in the section on two coupled cells is a particularly valuable tool for generating fixed patterns over a wide range of frequencies.

There are many indications that oscillatory behaviour is an important element in the activity of the brain [24] and even some indication that phase locking may play a role in visual processing [25]. It has been suggested [25, 26] that phase locking might be a way of correlating pattern recognition in different areas so that, for example, related images in different parts of the visual field can be grouped together. Some models of these behaviours have recently appeared [27].

The behaviour demonstrated here for a network of oscillators is associative memory through phase locking. The performance of the network for this task is very similar to that exhibited by Hopfield-type models although memory recognition is signalled by oscillatory rather than fixed-point behaviour. It is natural to ask what possible benefits might arise from using an oscillator network for phase-locking memory recall instead of the more conventional fixed-point attractor networks. One answer concerns

learning. In all network associative memories, the coupling matrix must be given a specific set of values corresponding to the memory patterns to be recalled. This is usually done using a learning procedure which modifies the coupling matrix while the network is placed in a learning mode of operation. The nature of this learning mode is mysterious, but in conventional network associative memories it is essential that it be separate and distinct from the normal operation of the memory. Otherwise, the network would continually be modifying its couplings in response to normal network activity even if the desired patterns were already learned correctly.

The oscillatory network memory offers a clear way of defining and initiated the learning mode of operation. Suppose that synaptic couplings are only plastic over a fairly long timescale. In other words, before the Hebb rule [18] or some other learning algorithm [4] can actually modify the synaptic strength, the pre- and postsynaptic cells must remain in given states of activity for a time period longer than the typical oscillation time of the network. In this case, no synaptic modification will take place during the normal memory recovery operation of the network. However, a learning mode could be inititiated by insuring that an input to be learned was presented for a time longer than the typical oscillatory period so that synaptic modification begins and conventional learning takes place. This could be accomplished by using the latching mode when $0 < a < \frac{1}{2}$ for the model cells [13]. Learning is initiated by adjusting a into this range. Thus, we see that the oscillator network naturally has two modes of operation. Signals presented while the network is in its operating mode ($\frac{1}{2} < a < 1$) cause associative recall of stored patterns through phase locking. While the network oscillates during its normal mode of operation no learning takes place. However, signals presented for prolonged periods due to cell latching when the network is in the learning mode ($0 < a < \frac{1}{2}$) will initiate synaptic modification.

Acknowledgments

I am extremely grateful to Eve Marder and the members of her lab, especially Jorge Golowasch and Jim Weimann, for patiently and skilfully introducing me to biological neurons and central pattern generators. I have also benefited from discussions with Tom Kepler, Nancy Kopell, Charlie Marcus and Steve Strogatz.

References

[1] McCulloch W S and Pitts W 1943 *Bull. Math. Biophys.* **5** 115
Little W A 1975 *Math. Biosci.* **19** 101
Hopfield J J 1982 *Proc. Natl Acad. Sci. USA* **79** 2554

[2] Hodgkin A L and Huxley A F 1952 *J. Physiol.* **117** 500
Hoppenstadt F C 1986 *An Introduction to the Mathematics of Neurons* (Cambridge: Cambridge University Press)

[3] Graubard K, Raper J A and Hartline D K 1983 *J. Neurophysiol.* **50** 508

[4] Amit D 1989 *Modelling Brain Function: The World of Attractor Neural Networks* (Cambridge: Cambridge University Press)
Abbott L F 1990 *Network* **1** 105

[5] Cohen A H, Rossignol S and Grillner S (eds) 1988 *Neural Control of Rythmic Movements in Vertebrates* (New York: Wiley)
Jacklet J W (ed) 1989 *Neuronal and Cellular Oscillators* (New York: Dekker)
Selverston A I and Moulins M (eds) 1987 *The Crustacean Stomatogastric System* (Berlin: Springer)

[6] Jack J J B, Noble D and Tsien R W 1983 *Electrical Current Flow in Excitable Cells* (Oxford: Clarendon)
[7] Horn D and Usher M 1989 *Phys. Rev.* A **40** 1036
[8] Wang L and Ross J 1990 *Proc. Natl Acad. Sci. USA* **87** 988
[9] Rinzel J 1990 *Proc. Int. Symp. on Mathematical Biology* ed E Teramoto (Berlin: Springer) to appear
[10] FitzHugh R 1961 *Biophys. J.* **1** 445
Nagumo J S, Arimoto S and Yoshisawa S 1962 *Proc. IRE* **50** 2061
[11] Van der Pol B 1927 *Phil. Mag.* **43** 700
[12] Grasman J 1987 *Asymptotic Methods for Relaxation Oscillators and Applications* (Berlin: Springer)
[13] Abbott L F 1990 *Proc. Natl Acad. Sci. USA* submitted
[14] Bélair J and Holmes P 1984 *Quart. J. Appl. Math.* 193
Storti D W 1984 Coupled relaxation oscillators: stability of phase-locked modes *PhD Thesis* Cornell University
Kawato M and Suzuki R 1980 *J. Theor. Biol.* **86** 547
[15] Feingold M, Gonzalez D L, Piro O and Viturro H 1988 *Phys. Rev.* A **A37** 4060
Rajasekar S and Lakshmanan M 1988 *Physica* **32D** 146
Wang W 1989 *J. Phys. A: Math. Gen.* **22** L627
[16] Winfree A T 1967 *J. Theor. Biol.* **16** 15
Kuramoto Y and Nishikawa I 1987 *J. Stat. Phys.* **49** 569
Ermentrout G B 1985 *J. Math. Biol.* **22** 1
Ermentrout G B and Kopell N 1984 *SIAM J. Math. Anal.* **15** 215
Dado H 1987 *Prog. Theor. Phys.* **77** 622
Kowalski J M, Ansari A, Prueitt P S, Dawes R L and Gross G 1988 *Complex Systems* **2** 441
[17] Kopell N and Ermentrout G B 1986 *Commun. Pure Appl. Math.* **39** 623
Hale J K 1969 *Ordinary Differential Equations* (New York: Wiley)
Guckenheimer J and Holmes P 1983 *Nonliner Oscillations Dynamical Systems and Bifurcations of Vector Fields* (Berlin: Springer)
[18] Hebb D O *The Organization of Behavior: A Neuropsychological Theory* (New York: Wiley)
[19] Amit D J, Gutfreund H and Sompolinsky H 1985 *Phys. Rev. Lett.* **55** 1530; *Phys. Rev.* A **32** 1007; *Phys. Rev.* A **35** 2293; 1987 *Ann. Phys.* **173** 30
[20] Kohonen T, Reuhkala E, Mäkisara K and Vainio L 1976 *Biol. Cybern.* **22** 159
Personnaz L, Guyon I and Dreyfus G 1985 *J. Physique* **46** L359
Kanter I and Sompolinsky H 1986 *Phys. Rev.* A **35** 380
[21] Gardner E, Stroud N and Wallace D J 1988 *Neural Computers* ed by R Eckmiller and C von der Malsburg (Berlin: Springer) p 251
Pöppel and Krey U 1987 *Europhys. Lett.* **4** 979
Krauth W and Mézard M 1987 *J. Phys. A: Math. Gen.* **20** L745
[22] Gardner E 1987 *Europhys. Lett.* **4** 481; 1988 *J. Phys. A: Math. Gen.* **21** 257
[23] Kepler T, Marder E and Abbott L F 1990 *Science* **248** 83
[24] Freeman W J 1978 *Elect. Clin. Neurophys.* **44** 369
Pöppel E and Logothetis N 1986 *Naturwissenshaften* **73** 267
Llinas R R 1988 *Science* **242** 1654
[25] Eckhorn R, Bauer R, Jordan W, Brosch M, Kruse W Munk M and Reitboeck H J 1988 *Biol. Cybern.* **60** 121
Grey C M and Singer W 1989 *Proc. Natl Acad. Sci. USA* **86** 1698
Grey C M, Kónig P, Engel A K and Singer W 1989 *Nature* **338** 334
[26] von der Malsburg C 1985 *Ber. Bunsenges Phys. Chem.* **89** 703
von der Malsburg C and Schneider W 1986 *Biol. Cybern.* **54** 29
[27] Li Z and Hopfield J J 1989 *Biol. Cybern.* **61** 379
Kammen D M, Inui M and Koch C 1990 *Snowbird Conference: Neural Networks for Computing* to appear
Kammen D M, Holmes P J and Koch C *Models of Brain Function* ed by Cotterhill R M J (Cambridge: Cambridge University Press)